metals

Article

Assessment of the Heat Input Effect on the Distribution of Temperature Cycles in the HAZ of S460MC Welds in MAG Welding

Jaromír Moravec *, Martin Švec, Šárka Bukovská and Jiří Sobotka

Department of Engineering Technology, Faculty of Mechanical Engineering, Technical University of Liberec, Studentská 1402/2, 46117 Liberec, Czech Republic; martin.svec@tul.cz (M.Š.); sarka.bukovska@tul.cz (Š.B.); jiri.sobotka@tul.cz (J.S.)

* Correspondence: jaromir.moravec@tul.cz; Tel.: +420-485-353-341

Abstract: Temperature cycles generated during welding have a significant effect on the changes in the HAZ of welds, regardless of whether these are changes in structure or mechanical properties; however, it is problematic to obtain temperature cycles with sufficient accuracy across the entire HAZ so that they can be generally taken and used in welding simulations and for real experiments of processes occurring in HAZ. In particular, for a study in a specific location, it is important to know the maximum temperature of the cycle and the cooling rate defined mainly by the parameter $t_{8/5}$. No studies in which anybody tries to find a mathematical description defining the basic parameters of temperature cycles in the HAZ could be found in the performed research. Therefore, the study presented in this paper results in a mathematical description defining the dependence of achieved maximum temperature on the distance from the fusion line in the HAZ of S460MC welds and with heat input values in the interval from 8 to 14 $kJ \cdot cm^{-1}$. Moreover, this paper presents the influence of heat input value on the weld pool geometry, including the effect of heat input value on grain coarsening in the highly heated HAZ.

Keywords: heat input; thermal cycle; thermal cell; heat affected zone; S460MC steel

Citation: Moravec, J.; Švec, M.; Bukovská, Š.; Sobotka, J. Assessment of the Heat Input Effect on the Distribution of Temperature Cycles in the HAZ of S460MC Welds in MAG Welding. *Metals* **2021**, *11*, 1954. https://doi.org/10.3390/met11121954

Academic Editor: Jacek Górka

Received: 16 November 2021
Accepted: 2 December 2021
Published: 5 December 2021

1. Introduction

In recent years, research teams have dealt with the issue of changes occurring in the HAZ of welds from high-strength fine-grained steels, including HSLA steels and steels hardened by quenching and tempering (Q-type), or steels for which normalizing rolling is essential (N-type). These are mainly studies where temperature cycles are applied to the testing sample using a thermal-mechanical simulators or other similar equipment; however, the basic approaches used in these studies are quite different. Many authors use their own shape of temperature cycles, where they mainly adjust the value of maximum temperature and own cooling to match the desired cooling parameter $t_{8/5}$ [1–7]. Typically, these authors apply a constant heating rate to the testing samples of chosen shape up to the desired maximum temperature followed by a constant cooling rate defined by the $t_{8/5}$ parameter [1,8], or a cooling part is divided into multiple constant rate intervals defined by the parameters $t_{T/8}$, $t_{8/5}$ and $t_{5/2}$ [2–5,7].

Furthermore, the authors use temperature cycles defined by employing equations or generated from the numerical simulations. For example, Lan et al. [1] used the so-called Rykalin mathematical model to determine the microstructure in HAZ. Thus, they generated a temperature cycle with a heating rate of 130 $°C \cdot s^{-1}$ to 1350 °C, holding for 2 s and then cooling with $t_{8/5}$ times of 30, 50, and 120 s. The Rykalin equation was also used by Marcell Gáspár [6], who used temperature-physical parameters obtained from programme JMatPro to define the temperature cycle but only for RT. The temperature cycles obtained by numerical simulation and their subsequent application to assess the structural changes were used in the work of Wang et al. [9]. In all cases mentioned above, these are studies about the effect of heat input value or cooling rate, showing what can happen to the testing material during welding. However, despite the very interesting results obtained, it is not easy to relate these results to a specific area of HAZ for the chosen process parameters and welding method.

In terms of assessing the properties of specific areas in HAZ, more advanced analyses were performed by the authors [10–12] using temperature cycles measured during real welding. In these cases, for a given welding method and process parameters, it is already possible to assess the properties of the specific area in HAZ regarding both the mechanical properties and structural changes. Boumerzouga et al. [10] used temperature cycles measured during MIG welding, with maximum temperatures close to 600, 780, 980, 1100 and 1250 °C; these cycles were subsequently applied by the device Smitweld TCS 1405 to assess the microstructural changes of steel AISI 1005 Mician et al. [11] used the temperature cycles measured during welding the steel S960MC using Gas Metal Arc Welding (GMAW). Measured and modified temperature cycles with a maximum temperature of 1105 °C were applied to employ the thermomechanical simulator Gleeble 3500 to the testing samples, observing the change in the mechanical and structural properties. The modification of the cycles consisted of changing the cooling rate, expressed by the parameter $t_{8/5}$. Moravec et al. [12] then used a temperature cycle with a maximum temperature of 1383 °C, measured during welding the steel S700MC by method GMAW, for physical simulations using the device Gleeble 3500. The study aimed to assess the welding effect on grain coarsening and the welding effect on the change of mechanical properties under different clamping stiffness conditions.

Analyses carried out by the authors [10–12] can already be assigned to a specific area in HAZ with sufficient accuracy; however, comprehensive information about the whole area's temperature distribution and the associated structural and mechanical properties cannot be done based only on these studies. Therefore, we present this study, which will allow the authors involved in the above studies to create temperature cycles from any part of HAZ for the GMAW welding method and heat input values from 8 to 14 $kJ \cdot cm^{-1}$. The study was carried out on steel S460MC, but the obtained results are applicable with sufficient accuracy to other HSLA steels because of the very similar thermal and physical properties. It will also be possible to use the generated temperature cycles to verify the results of the temperature-metallurgical analyses performed by the numerical simulations.

2. Materials and Methods

Steel S460MC (1.0982) is a structural, fine-grained, micro-alloyed and weldable steel produced by using thermomechanical rolling; it is steel with a minimum guaranteed yield strength (YS) of 460 MPa and good cold formability, while the ultimate tensile strength (UTS) of such material varies between 520 and 670 MPa. The steel is micro-alloyed by the elements such as Ti, Nb, Al and V. At the same time, it must be guaranteed that the sum of Nb, V and Ti content is no more than 0.22%. Table 1 shows the chemical composition defined by the standard EN 10149-2 and the chemical composition determined experimentally by using a Q4 Tasman spectrometer (Bruker, Berlin, Germany). The metallographic structure of the base material of S460MC steel is shown in Figure 1.

Table 1. Chemical composition (wt. %) of steel S460MC.

S460MC	C	Si	Mn	P	S	Cr	Mo	Ni
ČSN EN 10149-2	max. 0.12	max. 0.50	max. 1.60	max. 0.025	max. 0.015	-	-	-
experiment	0.072	0.012	1.324	0.031	0.008	0.011	0.002	0.006
	Cu	**Al**	**Ti**	**N**	**Nb**	**V**	**W**	
ČSN EN 10149-2	-	min. 0.015	max. 0.15	-	max. 0.09	max. 0.20	-	
experiment	0.020	0.031	0.004	0.006	0.051	0.080	0.039	

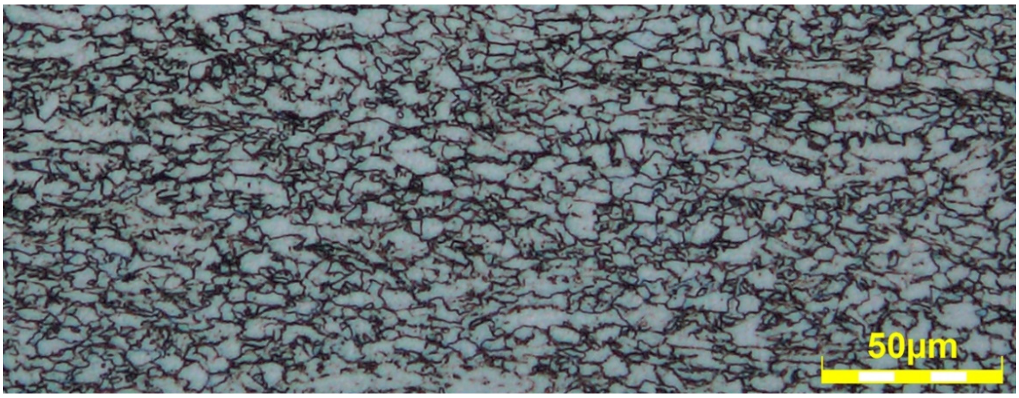

Figure 1. Metallographic structure of the base material—steel S460MC.

Since it was planned to assess the effect of temperature cycles with the different heat input values on grain coarsening, grain size analysis was first performed on the unaffected base material. The method EBSD determined the grain size on a Tescan Mira 3 (Tescan Orsay holding a.s., Brno, Czech Republic) scanning electron microscope (SEM). The Oxford Symmetry detector (Oxford Instruments, High Wycombe, UK) and the following process parameters were used for the EBSD analysis: high voltage HV = 15 kV, step size 0.7 µm and scanned area 1500 × 1500 µm. The EBSD method determined an average grain size of 9.97 µm. The result of the analysis with the illustration of the individual detected grains is shown in Figure 2. Table 2 shows the basic mechanical properties measured by the static tensile test and, in this case are results taken as an average from five measurements.

All welding experiments were carried out using the MAG method on a welding machine Migatronic BDH 550 Puls Sync (MIGATRONIC A/S, Fjerritslev, Denmark) connected to a linear automatic machine with continuously adjustable travel speed from 0.3 to 1.6 m·s^{-1}. OK Autrod 12.51 solid wire with a diameter of 1.2 mm was used as a filler material. As a shielding gas for the weld pool, an M21 mixed gas (82% Ar/18% CO_2) was used according to EN ISO 14175.

The welding was done in the PA position (according standard ISO 6947), where the torch axis was at a 90° angle regarding the base material, as schematically shown in Figure 3. The welding process was carried out under the synergy mode. A WeldMonitor (DIGITAL ELECTRIC, Brno, Czech Republic) with a data recording frequency of 20 kHz was used to monitor the actual process parameters. The distance of the welding nozzle from the welding area was set with a gauge of a distance Y, which was 15 mm during the initial experiments. Subsequently, the distance was reduced to 14 mm during the measurement of temperature cycles. In all cases, it was found that there was a globular transfer.

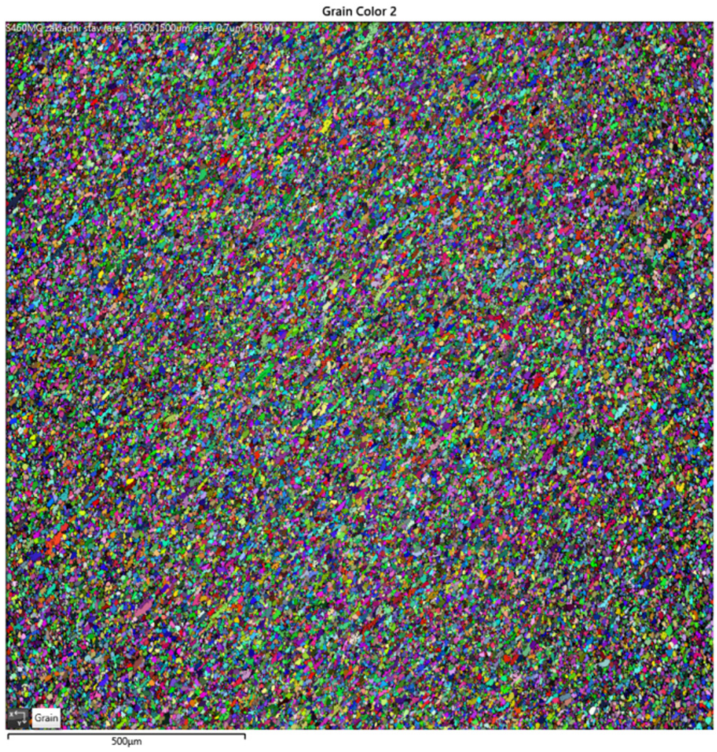

Figure 2. EBSD analysis of the base material.

Table 2. Basic mechanical properties of tested material—steel S460MC.

Mechanical Properties	Upper Yield Strength UpperYS [MPa]	Ultimate Tensile Strength UTS [MPa]	Uniform Ductility A_g [%]	Total Ductility A_{30} [%]
ČSN EN 10149-2	min. 460	520–670	x	min. 17
Measured values	544 ± 17	629 ± 21	13.15 ± 0.42	29.03 ± 0.91

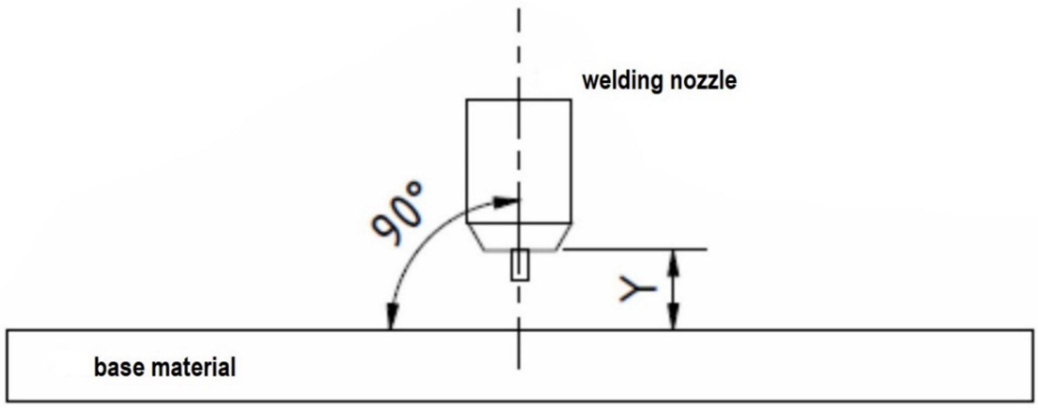

Figure 3. Adjustment of welding nozzle adjustment regarding the base material.

3. Influence of the Heat Input on the Weld Geometry

When measuring the temperature cycles with different maximum temperatures, it is necessary to know the weld pool geometry so that the thermocouples can be mounted at the required distances from the fusion line. Therefore, in the first phase of experiments, 7 welds with different heat input values from 8 up to 14 kJ·cm^{-1} were designed to describe the weld pool geometry. In particular, the welding current has a significant influence on the weld pool geometry, which is why it was decided to keep the same welding current and voltage values for all experiments and thus to achieve different heat input values only by changing the travel speed.

The welds were made on plates having dimensions 200 × 120 × 12 mm, as is shown in the schematic Figure 4. On each plate, two welds were made under the same parameters and distance between each other as 40 mm. The second weld was always performed after the sample had cooled down to the ambient temperature. Table 3 shows both the set values of current and travel speed for each weld and the actual values of process parameters measured by the WeldMonitor system.

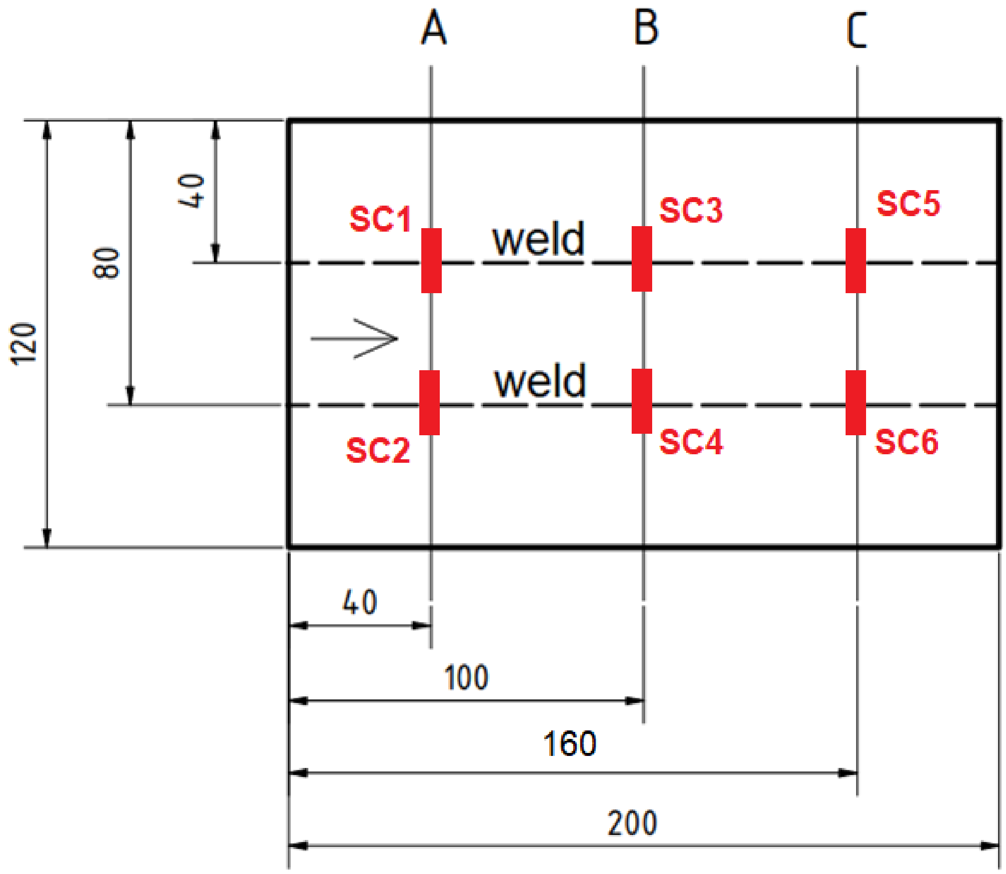

Figure 4. Locations of welds and areas for the metallographic scratch patterns.

Table 3. Set and actual process parameters of the individual types of welds.

Weld Designation	Set Parameters			Actual Parameters		
	Current [A]	Travel Speed [mm·min^{-1}]	Heat Input [kJ·cm^{-1}]	Travel Speed [mm·min^{-1}]	Voltage [V]	Current [A]
Weld_14	300	380	13.85	379	28.6	305.8
Weld_13	300	400	13.08	401	28.6	305.6
Weld_12	300	440	11.93	439	28.8	303
Weld_11	300	480	10.93	479	28.8	303
Weld_10	300	520	10.12	520	28.6	306.7
Weld_9	300	580	9.06	580	28.6	306.1
Weld_8	300	660	8.06	660	28.2	314.5

It is assumed that the constant cross-section area is already at a distance of 30 mm from the start and end of the weld. Therefore, for all seven types of welds (performed under different heat input values), metallographic scratch patterns were prepared in the locations shown in Figure 4. The microscopic evaluation of the weld geometry was performed by using a microscope Olympus (Olympus, Tokyo, Japan) and software NIS Elements AR 3.2 (Nikon, Tokyo, Japan). From the geometrical point of view, weld width, penetration depth and total weld area were always evaluated. For each weld type, 6 metallographic scratch patterns were evaluated. Thus, the average value of the geometric quantity could be determined, including the standard deviation—see Table 4. Figure 5 shows the average weld area vs. heat input value and Figure 6 is shown the penetration depth vs. heat input value, including the geometric deviations.

Table 4. Average values and standard deviations of the selected geometrical parameters.

Heat Input [kJ·cm^{-1}]	Weld	Average Weld Area [mm^2]	Average Weld Width [mm]	Average Penetration Depth [mm]
14	38–12	62.10 ± 1.66	13.91 ± 0.40	5.75 ± 0.11
13	40–12	59.22 ± 0.71	12.34 ± 0.24	5.69 ± 0.08
12	44–12	57.64 ± 1.69	11.83 ± 0.64	5.35 ± 0.11
11	48–12	52.48 ± 0.37	11.40 ± 0.57	5.11 ± 0.23
10	52–12	49.80 ± 1.86	10.49 ± 0.23	5.00 ± 0.20
9	58–12	42.32 ± 1.62	9.96 ± 0.18	4.53 ± 0.10
8	66–12	40.46 ± 0.62	10.51 ± 0.39	4.62 ± 0.14

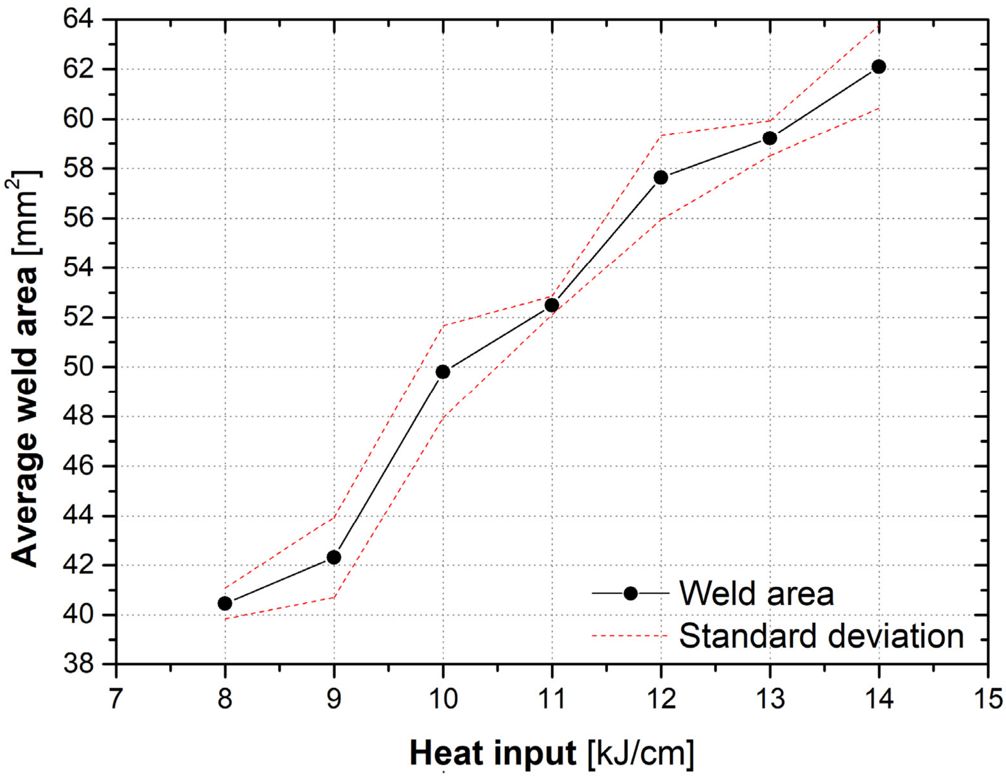

Figure 5. Average weld area vs. heat input values.

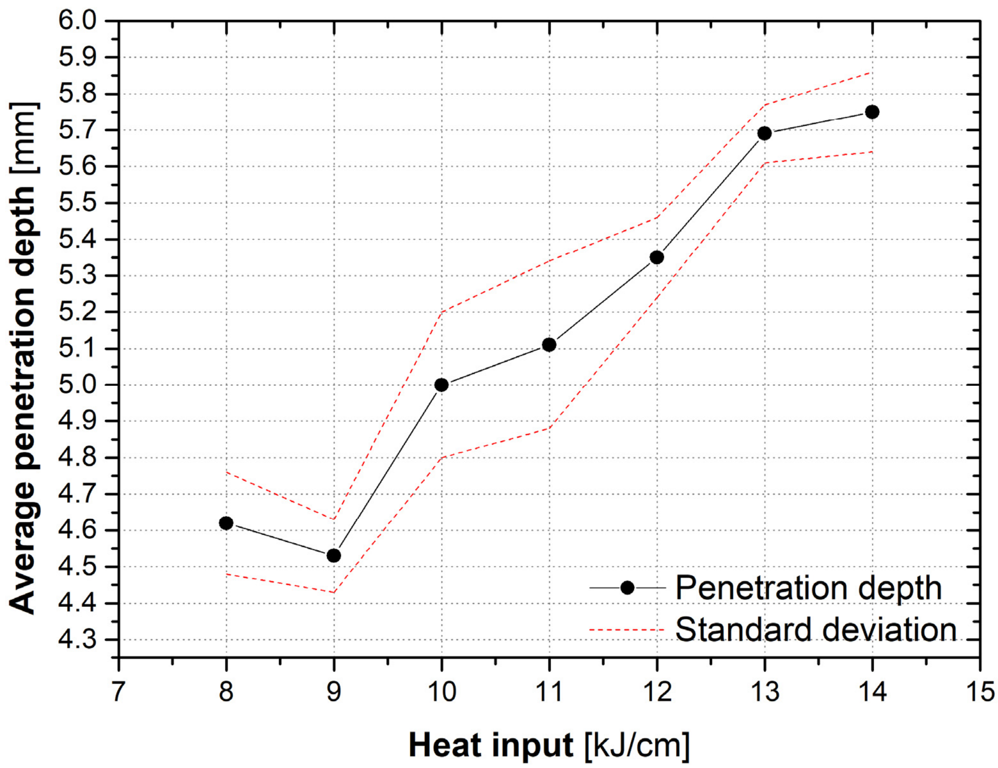

Figure 6. Penetration depth vs. heat input value.

4. Measurement of the Temperature Cycles

4.1. Preparation of Testing Samples

Welds with heat input values of 8 $kJ \cdot cm^{-1}$ and 14 $kJ \cdot cm^{-1}$ were selected for measuring the temperature cycles. These are the limit values used during the initial measurements and therefore there was expected that more significant differences could be found in the recorded temperature cycles. Two specially designed welding surface plates were prepared for the experiments, which differed from each other in the depth of holes milled for mounting TCs (thermocouples). The drawing of such testing welding surface plate with a heat input of 14 $kJ \cdot cm^{-1}$ (designated as variant A) is for illustration shown in Figure 7. This variant has holes milled to depths: 0.0, 0.2, 0.4, 0.6 and 0.8 mm from the predicted fusion line in the zone of maximum penetration. Variant B then has holes milled to depths 1.0, 1.2, 1.4, 1.6 and 1.8 mm from the predicted fusion line, again in the zone of maximum penetration. Testing plates for welds with a heat input value of 8 $kJ \cdot cm^{-1}$ were prepared the same way.

Thermocouples of S-type (PtRh10%—Pt) with conductors diameter of 0.35 mm were used to measure the temperature cycles up to 1600 °C, which is sufficient even if the thermocouple is directly poured by the weld metal. The ends of thermocouples were mutually stripped with a ceramic double tube and by the capacitor-discharge welding was welded to the bottom of holes in the testing plates.

After preparation and mounting the test plate to the welding jig, welds were made on the plate surface with parameters corresponding to the Weld 8 and Weld 14 as it is shown in Table 3—both for variant A and variant B. Table 5 shows the set and actual measured process parameters for each variant. Figure 8 shows the measured temperature cycles for a heat input value of 8 $kJ \cdot cm^{-1}$ for variant A. Measured maximum values of the temperature cycles varied from 1027 to 1665 °C, i.e., the particular thermocouples were already measuring the temperature in the melt. Figure 9 shows the measured temperature cycles for a heat input value 14 $kJ \cdot cm^{-1}$ for variant A. Measured maximum values of the temperature cycles varied from 782 to 1523 °C.

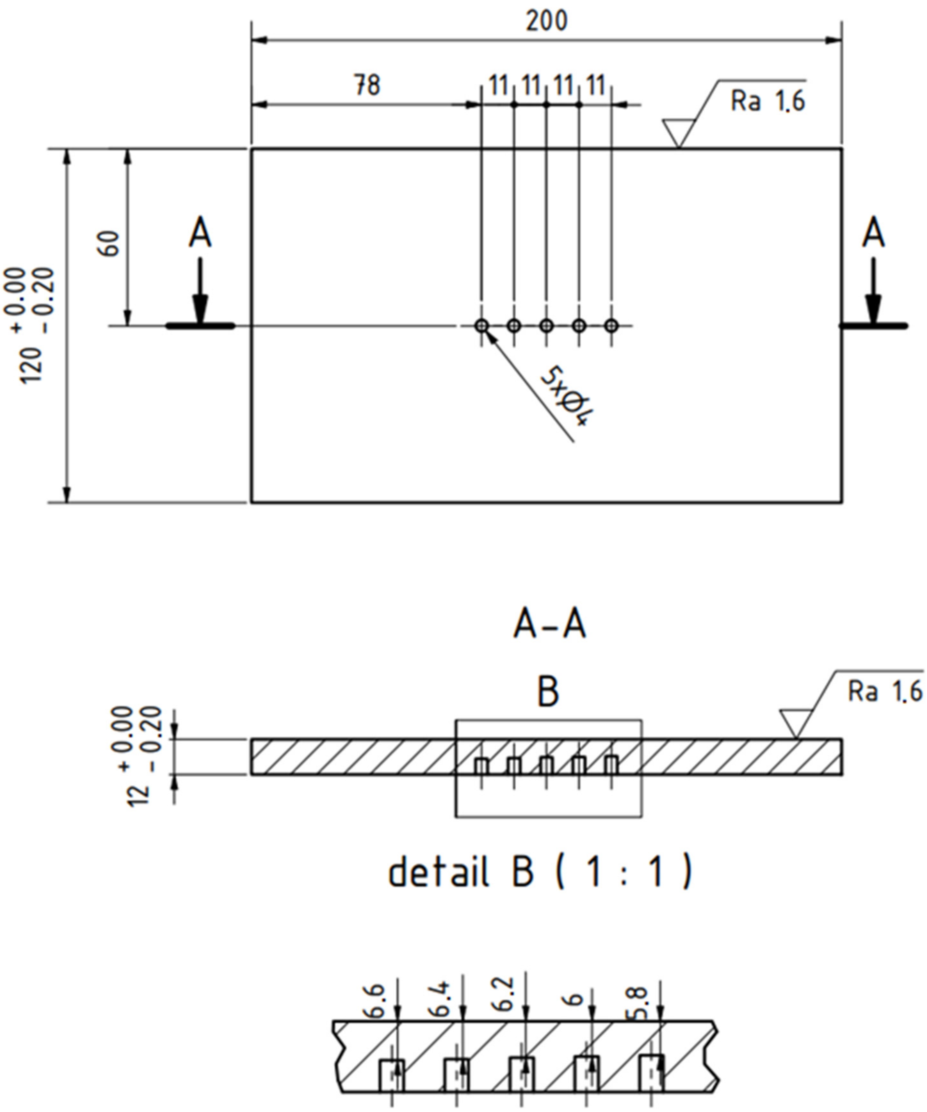

Figure 7. Designed testing sample for measuring the temperature cycles of welds with the heat input value 14 kJ·cm^{-1}.

Table 5. Process parameters of welds with heat input values 8 and 14 kJ·cm^{-1}.

Weld	Type of TC	Set Parameters		Actual Parameters			
		Current [A]	Travel Speed [mm·min^{-1}]	Heat Input Value [kJ·cm^{-1}]	Travel Speed [mm·min^{-1}]	Voltage [V]	Current [A]
Weld_14_A	S	300	380	13.90	379	304.8	28.8
Weld_14_B	S			13.87	380	307.2	28.6
Weld_8_A	S	300	660	8.01	660	310.2	28.4
Weld_8_B	S			7.96	659	308.0	28.4

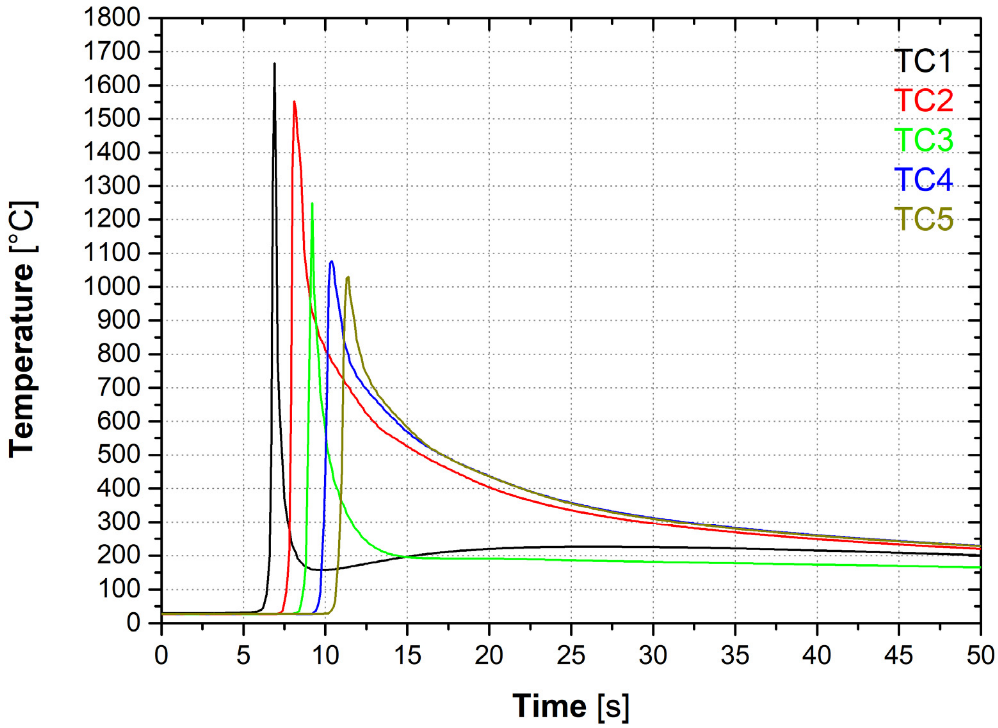

Figure 8. Temperature cycles measured in Weld_8_A.

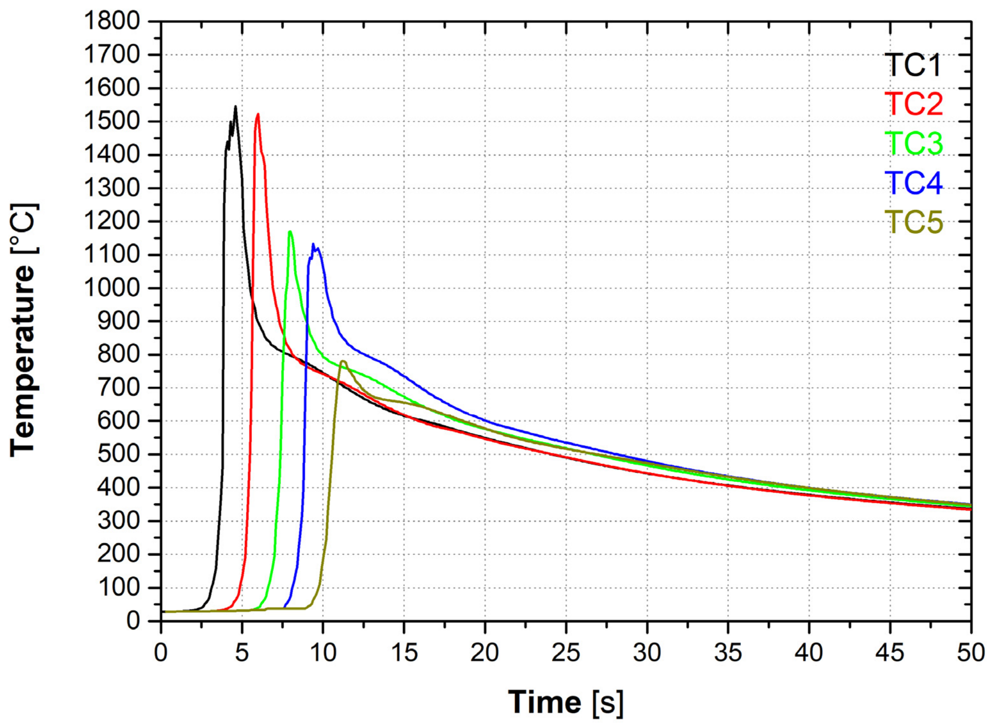

Figure 9. Temperature cycles measured in Weld_14_A.

4.2. Assignment of Temperature Cycles to the Specific Area in HAZ

First, it was necessary to confirm that the thermocouples were located within the expected distances from the fusion line, as found during the initial experiments. Therefore, a metallographic scratch pattern was made at the location of each TC. Due to the evaluation in the software NIS Elements AR 3.2, it was possible to determine the distance of thermocouples from the fusion line accurately. For Weld_8_A weld, the microscopic evaluation revealed that in the case of TC1 and TC2, melt penetrated right into the hole with TC, which was confirmed by the measured temperatures (well above 1500 °C). This happened due to the different heat removal in the hole for thermocouples. Thus, the temperature courses from TC1 and TC2 could not be used. After reaching the maximum temperature, TCs were separated from the melt and were not in contact with the material during cooling.

On the other hand, the temperature cycles measured by the Weld_8_A and Weld_8_B could already be used. For the same reason, TC1 could not be used for Weld_14_A and the other temperature cycles obtained from Weld_14_A and Weld_14_B could be used. Figure 10 already shows the temperature cycles measured at a heat input value of 8 kJ·cm^{-1}, where the individual cycles are mutually offset from each other. Hence, it corresponds to the actual distance from the fusion line. In the same way, the temperature cycles for a heat input value of 14 kJ·cm^{-1} are shown in Figure 11.

Subsequently, the points with the maximum temperature in each measurement cycle were fitted with the curve, approximated by the Boltzmann method. This provided a mathematical description of this curve (see Figure 12) and, therefore, a description of the temperature distribution curve in HAZ for weld with a heat input value of 8 kJ·cm^{-1}. In the same way, a mathematical description of the temperature distribution in HAZ for weld with a heat input of 14 kJ·cm^{-1} was obtained (see Figure 13).

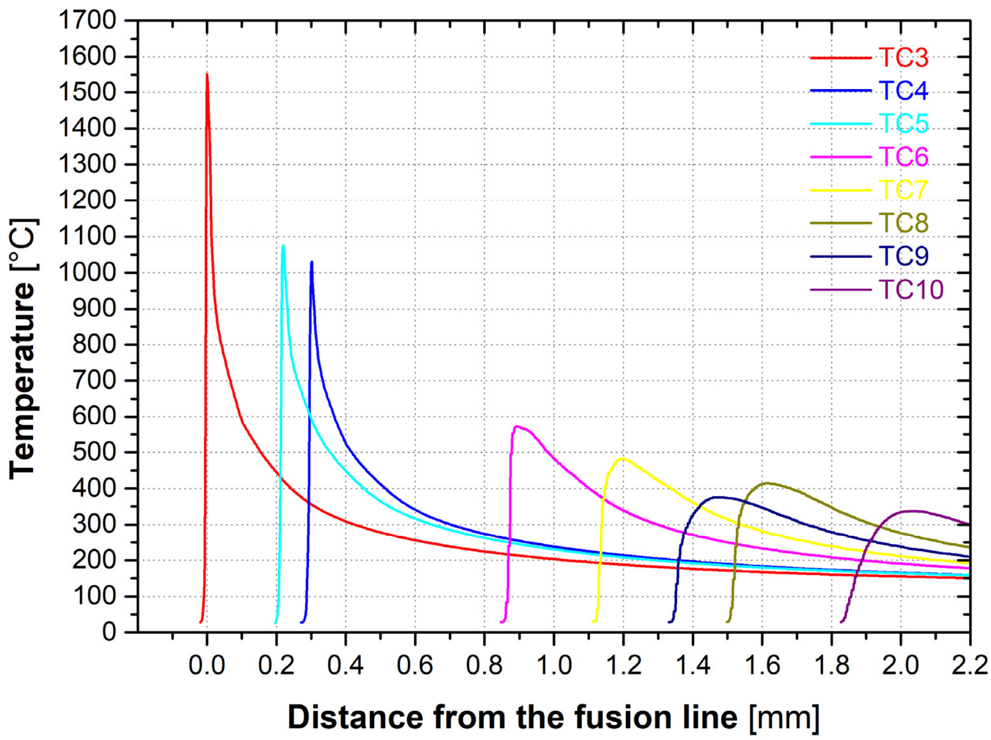

Figure 10. Temperature cycles (offset to correspond to the actual distance from the fusion line)—heat input value 8 kJ·cm^{-1}.

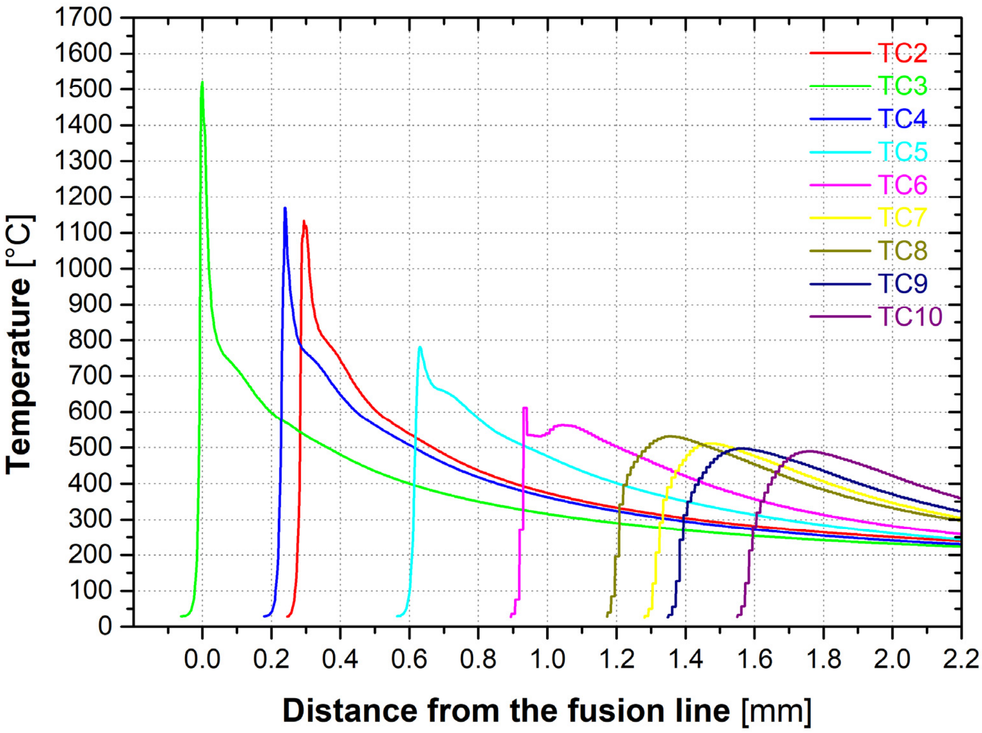

Figure 11. Temperature cycles (offset to correspond the actual distance from the fusion line)—heat input value 14 kJ·cm^{-1}.

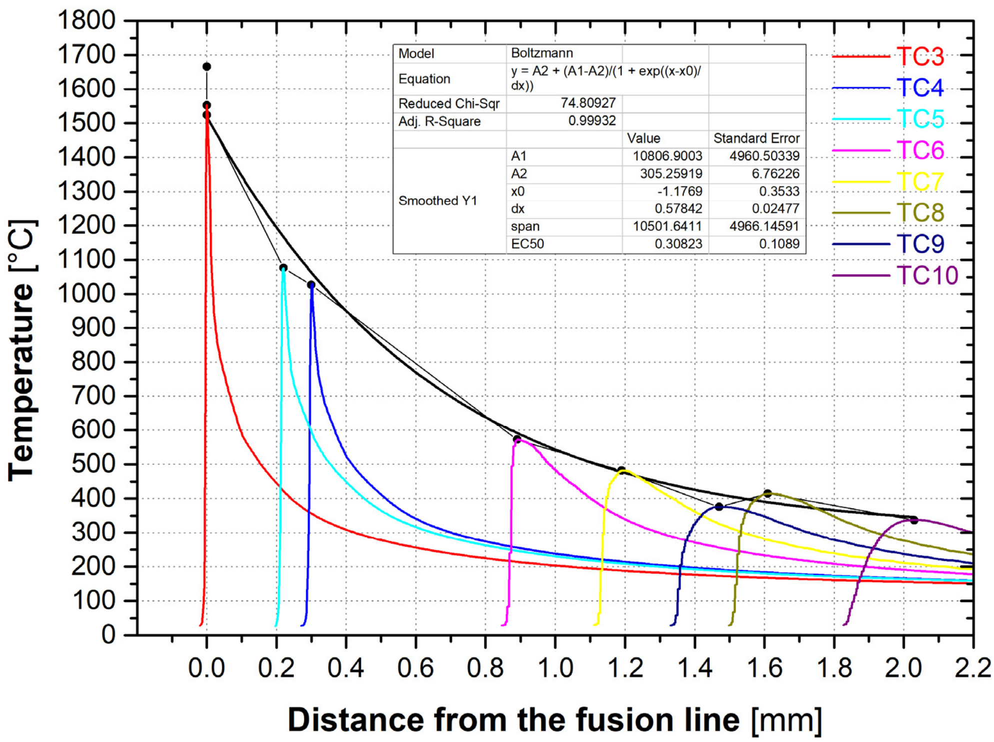

Figure 12. Mathematical description defining the temperature distribution in HAZ for weld with a heat input value 8 kJ·cm^{-1}.

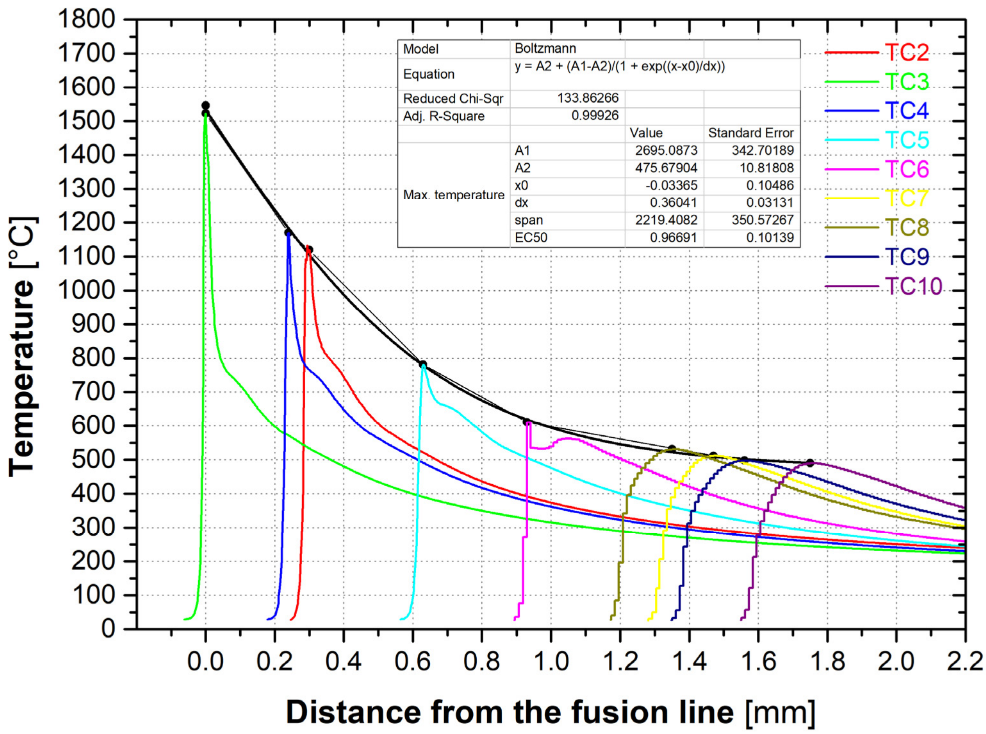

Figure 13. Mathematical description defining the temperature distribution in HAZ for weld with a heat input value 14 kJ·cm^{-1}.

5. Assessment of the Different Temperature Cycles Effect on Grain Coarsening

The mathematical description of temperature distribution in the HAZ for different heat input values made it possible to create temperature cycles corresponding to the same distance from the fusion line for steel S460MC. Thus, temperature cycles correspond to heat input values 8 and 14 kJ·cm^{-1}. The aim was to determine the effect of heat input on grain coarsening in the specific area of highly heated HAZ.

The temperature cycles used for comparison were designed to match a distance of 0.1 mm from the fusion line. A weighted average was used from the two measured cycles (the closest ones to this value) to create the resulting cycle with the maximum temperature corresponding to the mathematical description of temperature distribution in HAZ. Figure 14 is shown the method to obtain the temperature cycle for heat input values of 8 and 14 kJ·cm^{-1}, whereas both cycles are offset to each other on the time axis for clarity. The black dotted curve shows the measured temperature cycles closest to the generated cycle at 0.1 mm from the fusion line. The red curve shows the generated cycle for a heat input value of 8 kJ·cm^{-1} and the blue one shows the generated cycle of 14 kJ·cm^{-1}.

The obtained temperature cycles were then applied to the S460MC steel samples in the thermal-mechanical simulator Gleeble 3500 (Dynamic System Inc., New York, NY, USA) under a controlled force mode; the sample was not deformed during heating. The grain size was determined by the EBSD method on a scanning electron microscope Tescan Mira 3. For EBSD analysis was used a detector Oxford Symmetry with the same setting of parameters as for the analysis of the base material (Section 2). Results of EBSD analysis are shown in Table 6. A graphical result shows the individual detected grains for heat input value 8 kJ·cm^{-1} is shown in Figure 15a and for heat input value 14 kJ·cm^{-1} in Figure 15b.

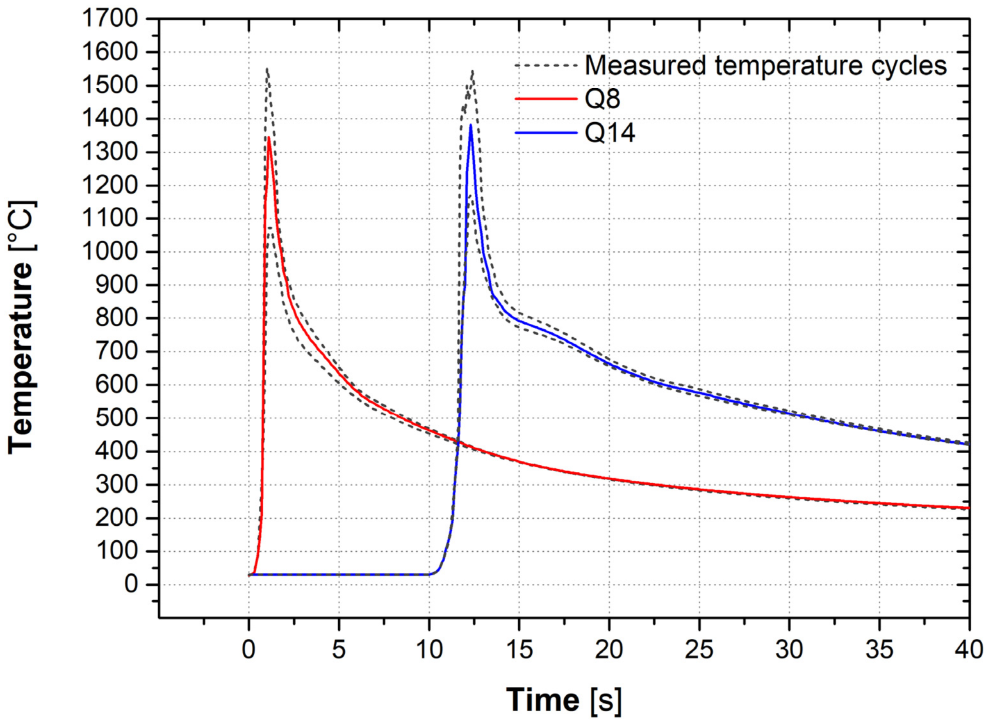

Figure 14. Temperature cycles for heat input values 8 and 14 kJ·cm^{-1} (generated in such manner to match with a distance of 0.1 mm from the fusion line).

Table 6. Results of grain coarsening measured by EBDS analysis.

Heat Input Value [kJ·cm^{-1}]	Max. Temperature of Cycle [°C]	Average Grain Size [µm]	Coarsening Compared to the Base Material [%]
Base material	-	9.97	0
Q8	1373	14.90	49.45
Q14	1386	15.20	52.46

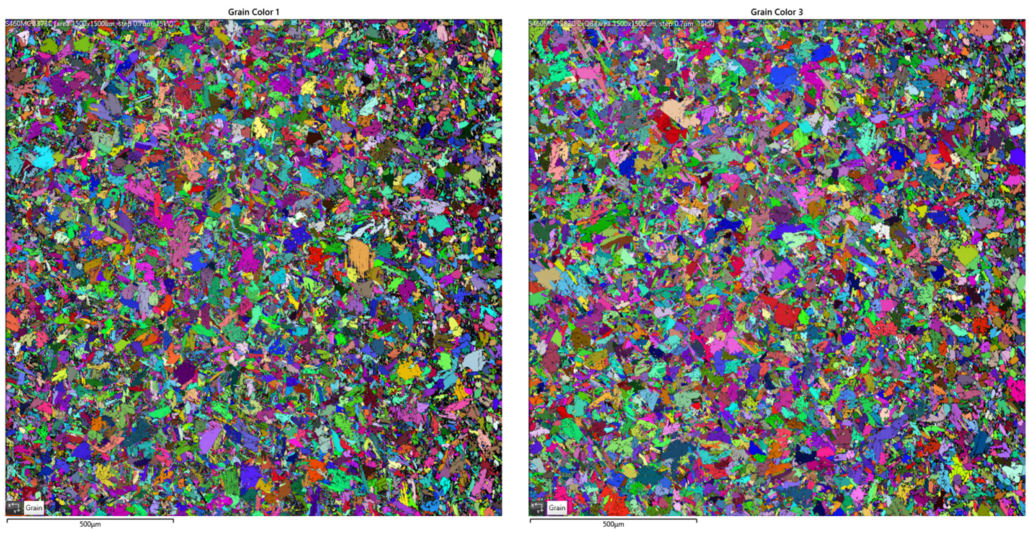

(**a**) (**b**)

Figure 15. Graphical result of EBSD analysis with the illustration of the individual detected grains (**a**)—heat input value 8 kJ·cm^{-1}; (**b**)—heat input value 14 kJ·cm^{-1}.

6. Discussion

It is quite difficult to assess the effect of heat input value on the changes that occur at specific areas of HAZ because the temperature distribution in HAZ is unknown. Moreover, using thermocouples to measure temperature cycles in a highly heated HAZ is problematic because the distance 0.1 mm of the thermocouple location from the fusion line generates more than 10% differences. While in the case of structural changes, both the maximum temperature and the course of the temperature cycle will play a significant role, the maximum reached temperature will be particularly crucial in the case of grain coarsening. Interesting results were obtained from the experiments and are discussed below.

The influence of the heat input value on the weld pool geometry is significant, especially for heat input values higher than 10 kJ·cm^{-1}. The higher heat input value, the larger weld width and penetration depth and thus, of course, also larger weld area, which is an expected effect. However, what is surprising is the relative stability of the weld geometric dimensions in the constant cross-section area. The maximum standard deviation in the penetration depth was lower than 5% and did not exceed 0.23 mm; however, even such small differences are significant enough in light of measuring temperature cycles in HAZ.

Information about the weld geometry for different heat input values allowed to design and use the special testing plates for measuring temperature cycles in specific areas of HAZ. Because of the high temperatures, it is necessary to use S-type thermocouples. However, the obtained heat cycles cannot be automatically assigned to a specific area of HAZ. This is due to the different heat removal in the hole for connection between the thermocouple and also to the variations mentioned above in values of the individual geometric quantities. Therefore, for each location of TC, it is necessary to experimentally verify the actual distance of thermocouples from the fusion line employing micro-scratch patterns.

Due to this, it was possible to assign individual temperature cycles to the specific area of HAZs, as shown in Figure 10 for a heat input value of 8 kJ·cm^{-1} and Figure 11 for a heat input value of 14 kJ·cm^{-1}. By coupling the temperature cycles at locations of the maximum temperature, it was possible to use the Boltzmann approximation to obtain the temperature distribution in HAZ as a function of the heat input value. The temperature distribution in HAZ of welds made by method GMAW on steel S460MC can be described by Equation (1) for a heat input value 8 kJ·cm^{-1} and Equation (2) for a heat input value 14 kJ·cm^{-1}.

$$y = 305.3 + \frac{10,501.6}{1 + e^{\frac{x+1.177}{0.578}}} \tag{1}$$

$$y = 475.7 + \frac{2219.4}{1 + e^{\frac{x+0.034}{0.36}}} \tag{2}$$

where:

x—is the distance from fusion line (mm);
y—is the maximal temperature for the given distance from fusion line (°C).

Equations (1) and (2) represent the limits of the temperature distribution interval in HAZ for heat input values from 8 to 14 kJ·cm^{-1}. The weighted average method can determine the temperature distribution in HAZ for heat input within the interval with sufficient accuracy. A graphical comparison of the temperature distribution in HAZ using Equations (1) and (2) is shown in Figure 16. From this figure, it is clear that the maximum temperatures in the HAZ decrease faster for lower heat input values and the width of HAZ is lower. At the same time, it can be stated that differences in the maximum temperatures distribution are very small in the interval 1500–700 °C and the effect of heat input is only more pronounced below 700 °C, i.e., from approximately 0.7 mm from the fusion line. For HAZ at distances from 0.1 to 0.7 mm from the fusion line, the difference between the maximum temperatures obtained for the heat input values of Q = 8 and Q = 14 kJ·cm^{-1} varied from 2.5% up to 4.2%. Beyond this value, more significant deviations occur. For a distance of 0.8 mm from the fusion line, the difference is already 5.2% and for a distance of 0.9 mm from the fusion line, the difference between the temperatures is 6.6%.

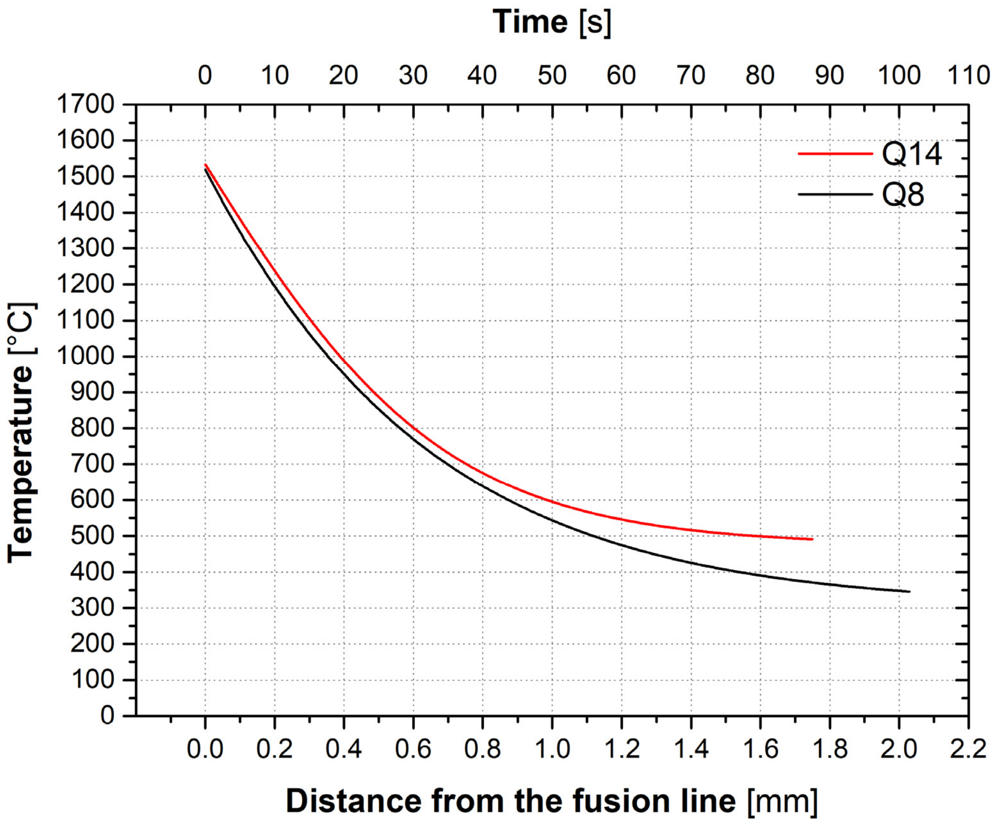

Figure 16. Comparison of the maximum temperatures distribution in HAZ as a function of the heat input value.

The third phase of experiments was aimed at assessing the effect of temperature cycles on grain size changes in HAZ. For this purpose, temperature cycles were generated using a mathematical description of temperature distribution curves in HAZ and having shape according to the heat input value—see Figure 14. These cycles were subsequently applied to the S460MC fine grain steel samples. Thus, the difference in the maximum cycle temperature was very small—about 13 °C. However, the more significant difference was detected in the own shape of the temperature cycle, especially at temperatures below 850 °C.

EBDS analysis confirmed the grain coarsening. For the temperature cycle corresponding to a heat input value of 8 kJ·cm^{-1}, the grain coarsened by 49.5%. For the temperature cycle corresponding to a heat input value of 14 kJ·cm^{-1}, the grain coarsened by 52.5% compared to the base material. The obtained results confirm that, in highly heated HAZ, the difference between the maximum temperatures determined at different heat input values is small. Thus, the differences in grain coarsening intensity will be small.

7. Conclusions

The study described in this paper aimed to comprehensively assess the distribution of maximum temperatures in HAZ as a function of the heat input value during GMAW welding. The study was carried out on material S460MC, but the obtained results can be applied with sufficient accuracy to other HSLA steels because of the very similar thermo-physical properties. It will also be possible to use the generated temperature cycles to verify the thermal-metallurgical analyses results performed by numerical simulations.

Based upon the performed experiments and obtained results, the following conclusions can be drawn:

(1) The heat input has a significant effect on the weld deposit geometry—the higher heat input value, the higher width, weld deposit and weld area. For heat input within the

range 8–14 kJ·cm^{-1}, high geometric stability was achieved in the steady-state welding zone with deviations from the mean value lower than 5%.

(2) For correct mapping of the temperature distribution in HAZ, it is necessary to use S-type thermocouples. At the same time, however, considerable attention must be paid to the method of its placement and especially to the determination of its actual distance from HAZ. Even a very small deviation in measuring such distance can significantly affect the predicted temperature distribution in a highly heated HAZ.

(3) Equations (1) and (2) can be used to describe the temperature distribution in HAZ of welds made by the MAG method on steel S460MC for heat input values 8 and 14 kJ·cm^{-1}. At the same time, it can be assumed that these equations can be applied with sufficient accuracy to steels with similar thermal physical properties.

(4) To describe the temperature distribution in HAZ of welds with heat input values varying within the interval 8 and 14 kJ·cm^{-1}, the approximation of Equations (1) and (2), or the weighted average method, can be used with sufficient accuracy.

(5) The shape of the temperature cycles is similar under temperatures above 850 °C, regardless of the heat input value. The effect of the heat input is only strongly evident below 850 °C, where the parameter $t_{8/5}$ plays a significant role.

(6) Temperature cycles belonging in the highly heated HAZ have a significant effect on grain coarsening, at least for steel S460MC steel. In particular, the maximum reached temperature reached is very important in this case. The application of temperature cycles with a maximum temperature of about 1380 °C, corresponding to the area in HAZ with distance of 0.1 mm from the fusion line, resulted in a grain coarsening by about 50%.

(7) However, the higher heat input value did not cause significant grain coarsening. The difference in grain coarsening caused by the temperature cycles with heat input values 8 and 14 kJ·cm^{-1} was only 3%.

Author Contributions: Conceptualization, J.M. and M.Š.; methodology M.Š.; investigation, J.M., M.Š. and Š.B.; resources, J.M.; data curation, M.Š. and Š.B.; writing—original draft preparation, J.M.; writing—review and editing, M.Š., Š.B. and J.S.; visualization, Š.B.; supervision, J.M.; funding acquisition, Š.B.; All authors have read and agreed to the published version of the manuscript.

Funding: This research was funded by the Student Grant Competition of the Technical University of Liberec under the project No. SGS-2020-5008 "Influence of residual stresses during technological processing on fatigue life of manufactured parts".

Institutional Review Board Statement: Not applicable.

Informed Consent Statement: Not applicable.

Data Availability Statement: Not applicable.

Conflicts of Interest: The authors declare no conflict of interest.

References

1. Lan, L.; Shao, G. Morphological Evolution of HAZ Microstructures in Low Carbon Steel during Simulated Welding Thermal Cycle. *Micron* **2020**, *131*, 102828. [CrossRef] [PubMed]
2. Shi, Y.; Han, Z. Effect of Weld Thermal Cycle on Microstructure and Fracture Toughness of Simulated Heat-Affected Zone for a 800 MPa Grade High Strength Low Alloy Steel. *J. Mater. Process. Technol.* **2008**, *207*, 30–39. [CrossRef]
3. Górka, J. Influence of the Maximum Temperature of the Thermal Cycle on the Properties and Structure of the HAZ of Steel S700MC. *IOSR J. Eng.* **2013**, *3*, 22–28. [CrossRef]
4. Żuk, M.; Górka, J.; Jamrozik, W. Simulated Heat-Affected Zone of Steel 4330V. *Mater. Perform. Charact.* **2019**, *8*, 606–613. [CrossRef]
5. Guo, J.; Xu, X.; Jepson, M.A.; Thomson, R.C. Influence of Weld Thermal Cycle and Post Weld Heat Treatment on the Microstructure of MarBN Steel. *Int. J. Press. Vessel. Pip.* **2019**, *174*, 13–24. [CrossRef]
6. Gáspár, M. Effect of Welding Heat Input on Simulated HAZ Areas in S960QL High Strength Steel. *Metals* **2019**, *9*, 1226. [CrossRef]
7. Kik, T.; Górka, J.; Kotarska, A.; Poloczek, T. Numerical Verification of Tests on the Influence of the Imposed Thermal Cycles on the Structure and Properties of the S700MC Heat-Affected Zone. *Metals* **2020**, *10*, 974. [CrossRef]

8. Zavdoveev, A.; Rogante, M.; Poznyakov, V.; Heaton, M.; Acquier, P.; Kim, H.S.; Baudin, T.; Kostin, V. Development of the PC-GMAW Welding Technology for TMCP Steel in Accordance with Welding Thermal Cycle, Welding Technique, Structure, and Properties of Welded Joints. *Rep. Mech. Eng.* **2020**, *1*, 26–33. [CrossRef]
9. Wang, Y.; Ding, M.; Zheng, Y.; Liu, S.; Wang, W.; Zhang, Z. Finite-Element Thermal Analysis and Grain Growth Behavior of HAZ on Argon Tungsten-Arc Welding of 443 Stainless Steel. *Metals* **2016**, *6*, 77. [CrossRef]
10. Boumerzoug, Z.; Raouache, E.; Delaunois, F. Thermal Cycle Simulation of Welding Process in Low Carbon Steel. *Mater. Sci. Eng. A* **2011**, *530*, 191–195. [CrossRef]
11. Mičian, M.; Harmaniak, D.; Nový, F.; Winczek, J.; Moravec, J.; Trško, L. Effect of the T8/5 Cooling Time on the Properties of S960MC Steel in the HAZ of Welded Joints Evaluated by Thermal Physical Simulation. *Metals* **2020**, *10*, 229. [CrossRef]
12. Moravec, J.; Novakova, I.; Sobotka, J.; Neumann, H. Determination of Grain Growth Kinetics and Assessment of Welding Effect on Properties of S700MC Steel in the HAZ of Welded Joints. *Metals* **2019**, *9*, 707. [CrossRef]